Asian Journal of Chemistry; Vol. 26, No. 2 (2014), 383-388

ASIAN JOURNAL OF CHEMISTRY

http://dx.doi.org/10.14233/ajchem.2014.15404

Production of Hydrogen from Ethanol Steam Reforming Over Ni-Mn/La_2O_3-ZrO_2 Catalyst

HONGDA WU*, YU YIN, HANZHI LIU, TIANSHI LIU and LUE ZHAO

College of Biological and Chemical Engineering, Guangxi University of Science and Technology, Liuzhou 545006, P.R. China

*Corresponding author: E-mail: whongda@126.com

Received: 1 March 2013; *Accepted*: 9 July 2013; *Published online*: 15 January 2014; AJC-14548

La_2O_3-ZrO_2 composite oxide support was prepared by oxalate precipitation method and Ni-Mn/La_2O_3-ZrO_2 catalysts were prepared by impregnation. The catalysts were characterized by means of X-ray diffraction, temperature programmed reduction and temperature programmed oxidation. The performance of catalysts in steam reforming of ethanol was studied and the effects of the catalyst composition on catalytic activity and selectivity were discussed. The results showed that Ni-Mn/La_2O_3-ZrO_2 catalyst was remarkable tetragonal phase, nickel species and manganese species were highly dispersed on the support surface. The Ni active component existed as zero valent in catalysts while Mn active component existed as MnO during steam reforming of ethanol and synergy existed between nickel and manganese species; (8Ni1Mn)4(2La8Zr) catalyst exhibited the best catalytic performance in steam reforming of ethanol, with which ethanol conversion rate was 100 % in the situation of 823 K and CO content was lower at high temperature. A certain amount of carbon deposition was observed on all Ni-Mn/La_2O_3-ZrO_2 catalysts in steam reforming of ethanol.

Keywords: Ethanol, Hydrogen production, Nickel, Manganese, Carbon deposition, Stability.

INTRODUCTION

It is (an) inevitable trend that use of fossil fuel transform into sustainable developing and pollution-free non-fossil energy. The superiority of hydrogen production from steam reforming of ethanol is drawing more and more attention of researchers[1] and ethanol has become the preferred materials for production of hydrogen[2]. Literature[3,4] indicated that Ni had high ability in breaking C-C bond and relatively high catalytic activity in steam reforming of ethanol, but also shortages such as higher CH_4 and CO content in gas phase product and catalyst's easy-carbon deposits. In recent years, researches on multicomponent non-precious metal catalysts applying in hydrogen production from steam reforming of ethanol have gained great achievements.

Previous studies[5-7] have shown that, no carbon deposition existed on Cu-based catalyst using Mn as accessory ingredient, $Ni/Ce_{0.75}Zr_{0.25-x}Mn_xO_2$ catalyst and Co-Mn/ZnO catalyst and the catalysts maintain a stable catalystic activity. In studies of Torres and his coworkers[8] catalytic activity of Ni/La_2O_3-Al_2O_3 and Mn-Co/ZnO in steam reforming of ethanol under mid temperature were compared. The research shows that, a CoO revivification was promoted after joining Mn in Co based catalyst, coming with Co and Mn double metal grain, which endows Mn-Co/ZnO catalyst with medium temperature steam reforming of ethanol activity. Zhou and coworkers[9] studied the behavour of Cu-Ce-Mn-O catalyst in ether steam reforming. After characterized by XRD, XPS and XAFS, they found that the adjunction of Mn species improved the dispersion degree, revivification ability and increased the quantity of active sites. Also it markedly promoted the producion of hydrogen and obtained higher CO_2 selectivities and lower CO selectivity. Papavasiliou *et al.*[10] found that Cu-Ce-O and Cu-Mn-O catalyst had excellent catalytic function in oxidation and steam reforming of ethanol, also lower the content of harmful outcome of CO. Casanovas and coworkers[11] studied the promoting effects of Ni on Cu/ZnO samples catalyzing ethanol sream reforming as well as WGS conversion. X-ray diffraction and other characterization shown that the cellular structure Co-Mn/ZnO powder catalyst has provided positive effects on low-temperature steam reforming of ethanol and WGS conversion because of the advantage Mn has in redox conversion of oxydic Co and reductive Co. Berman and coworkers[12] obtained multi-component catalyst after adding manganic ingredient in Ru/Al_2O_3. X-ray diffraction and temperature programmed reduction shown that MnO_2 transfered to Mn_3O_4 and Spinel phase $MnAl_2O_4$ under the reaction condition. In methanol steam reforming system, Mn as accelerant had little influence on catalyst activity of Ru/Al_2O_3, while heat stability of catalyst was increased at a high temperature (kept in activity at 1373 K). The reason for it was that $MnAl_2O_4$ and manganese oxide restrain the migration of active component Ru atom, thus the sintering of Ru grain can be controlled.

In conclusion, Mn can improve the activity of the metal dispersion and play a synergy role, which makes catalyst exhibits better activity stability and selectivity. Take it into account that nickel-based catalysts possess strong C-C bond cleavage ability, but has high CO and CH_4 content in catalyst product of steam reforming of ethanol. The activity and selectivity of the catalysts might be improved, if add Mn as cocatalyst. So we made La_2O_3-ZrO_2 as a carrier, prepared a series of Ni-Mn/La_2O_3-ZrO_2 catalysts. The catalysts are characterized by temperature programmed reduction and temperature programmed oxidation to identify the surface property and further research of their catalytic properties in steam reforming of ethanol was then conducted.

EXPERIMENTAL

$Zr(NO_3)_4 \cdot 5H_2O$, $La(NO_3)_3 \cdot 6H_2O$, $Ni(NO_3)_2 \cdot 6H_2O$, $Mn(NO_3)_2$ solution, $(NH_4)_2C_2O_4 \cdot H_2O$, anhydrous ethanol, *etc.* were used in present study.

WFS-3015 Catalytic Evaluation Device, SP-6800A Gas Chromatograph; DX-2700 X-ray Diffractometer (Dandong fangyuan instrument Co.LTD of China), Cu target, operating at voltage and current of 40 KV and 30 mA; PCA-1100 Chemical Adsorption Analyzer (Beijing Builder electronic technology Co. Ltd).

Preparation of catalyst: 0.5 mol L^{-1} ammonium oxalate solution and the mixed solution of $Zr(NO_3)_4$ and $La(NO_3)_3$ with a total metal ion concentration of 0.5 mol L^{-1} were parallel flowed into a baker with the act of stirring, then left for 12 h and filtered. The precipitation was obtained through adding into dehydrated ethanol and stirring the solid until it become fully decentralized, then filtered and dried.

Lanthanum oxide and zirconium oxide composite support (La:Zr = 2:8) can be obtained after calcining the precipitation for 3 h at 973 K in air atmosphere. Impregnated La_2O_3 and ZrO_2 composite powder in $Ni(NO_3)_2$ and $Mn(NO_3)_2$ solution and stirred, dried and calcined at 973 K for 3 h. Loaded active ingredient of Ni and Mn by dipping method, then a series of Ni-Mn/La_2O_3-ZrO_2 catalysts would be obtained (labeled according to atomic ratio): (8Ni1Mn)4(2La8Zr), (6Ni1Mn)4(2La8Zr), (4Ni1Mn)4(2La8Zr), (2Ni1Mn)4 (2La8Zr) and (1Ni1Mn)4(2La8Zr) catalyst.

Evaluation of catalyst activity: The catalytic experiments were performed in a continuous fixed bed reactor in normal pressure (lined with quartz glass tube). Prior to reaction, 0.5 g of fresh powder catalyst was placed in the reactor and reduced *in situ* at 873 K for 2h under a H_2-Ar flow of 30 mL/min, then adjust to the reaction temperature under the H_2-Ar flow. The ethanol and water mixture with C_2H_5OH:H_2O = 1:6(n/n) was introduced to the reactor by using a pump at a rate of 0.1 mL/min and vaporized at 200 ºC, then mix with 30 mL/min Ar flow in the fixed bed reactor. The reaction products were cooled in thermostatic circulator at 2 ºC and analyzed by two on-line gas chromatographs. Made non-condensable gas mixture into the SP-6800A equipped with a TCD and carbon molecular sieves columns to be analyzed. Made the cooling liquid in the liquid phase mixture into the SP-6800A equipped with a FID and AE.FFAP capillary column to be analyzed. Then we had data processing on a Qianpu chromatography workstation.The ethanol conversion rate(X), acetaldehyde selectivity and acetone selectivity is calculated as follows:

$$X = \left(\frac{n_1}{n_0}\right) \times 100\ \%$$

$$S_{Nn} = \left(\frac{3n_2}{2n_1}\right) \times 100\ \%$$

$$S_{YN} = \left(\frac{n_3}{n_1}\right) \times 100\ \%$$

n_o: Amount of ethanol entering the reactor, mol, n_1: Amount of ethanol that reaction comsued, mol, n_2: Amount of acetone produced in reaction, mol, n_3: Amount of acetaldehyde produced in reaction, mol.

Characterization of catalysts

X-Ray diffraction: XRD patterns were collected on a DX-2700 X ray diffractometer, equipped with a rotating anode and Cu K radiation source. Diffractograms were recorded in the 10-80º range of 2θ with a step of 0.02(º)/min, operating voltage 40 kV and current 30 mA.

Temperature programmed reduction: Temperature programmed reduction measurement was conducted with the support of Chemical adsorption analyzer instrument (PCA-1100). About 200 mg fresh catalyst were loaded in quartz-U-type reactor with an inner diameter of 4 mm and heated from room temperature to 923 K at a heating rate of 10 K/min in a stream of O_2 and cooled down to room temperature in Ar flow, then heated from room temperature to 1123 K at a heating rate of 10 K/min when baseline was steady in molecular sieve-purified stream of 5 % H_2 in Ar (40 mL/min).

Temperature programmed oxidation: Temperature programmed oxidation measurement was conducted with the support of Chemical adsorption analyzer instrument (PCA-1100). About 200 mg catalyst used by reforming reaction were loaded in quartz-U-type reactor with an inner diameter of 4 mm and heated from room temperature to 923 K at a heating rate of 10 K/min in a stream of H_2, then cooled down to room temperature in Ar flow, then heated from room temperature to 1123 K at a heating rate of 10 K/min when baseline was steady in molecular sieve-purified stream of 3 % O_2 in Ar (40 mL/min).

The temperature programmed rduction and temperature programmed oxidation were performed with a conventional setup equipped with TCD detector.

RESULTS AND DISCUSSION

Catalytic XRD characterization: The catalyst was characterized by X-ray diffraction technology and Fig. 1 shows the XRD patterns of the catalysts. Fig. 1 showed the strong characteristic diffraction peak of tetragonal phases ZrO_2 (2θ value = 29.8, 34.5, 49.7, 58.5º; PDF#42-1164) can be observed not only in all XRD patterns of Ni-Mn/La_2O_3-ZrO_2 catalysts prepared by impregnation method, but also in all the patterns of the catalysts which have been used in catalytic ethanol steam reforming. This result illustrates that carrier structure is stable during catalytic reaction.

In addition to strong characteristic diffraction peak of tetragonal phases ZrO_2 (2θ value = 29.8, 34.5, 49.7 and 58.5º;

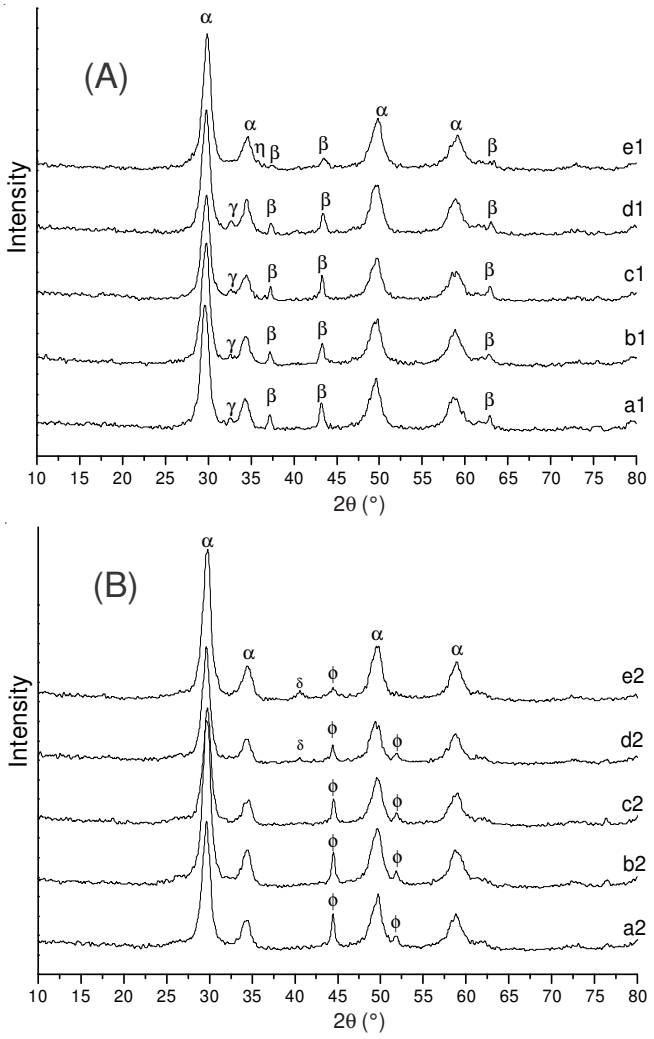

α: ZrO_2, β: NiO, γ: Mn_2O_3, η: $Mn_{0.994}Mn_{2.001}O_4$, Φ: Ni, δ: MnO

Fig. 1. XRD patterns of Ni-Mn/La_2O_3-ZrO_2 catalysts with different Ni/Mn ratio. a1 (8Ni1Mn)4(2La8Zr) fresh catalyst, a2 (8Ni1Mn)4(2La8Zr) catalyst used, b1 (6Ni1Mn)4(2La8Zr) fresh catalyst b2 (6Ni1Mn)4(2La8Zr) catalyst used, c1 (4Ni1Mn)4(2La8Zr) fresh catalyst c2 (4Ni1Mn)4(2La8Zr) catalyst used, d1 (2Ni1Mn)4(2La8Zr) fresh catalyst d2 (2Ni1Mn)4(2La8Zr) catalyst used, e1 (1Ni1Mn)4(2La8Zr) fresh catalyst e2 (1Ni1Mn)4(2La8Zr) catalyst used

PDF#42-1164), rhombohedral phase NiO crystal diffraction peak (2θ value = 37.3, 43.3, 62.9º; PDF#44-1159) could be observed in all fresh catalysts. But the intensity of NiO diffraction peak reduced with Ni/Mn proportion decreased and only weak rhombohedral phase NiO crystal diffraction peak existed in (1Ni1Mn)4(2La8Zr) catalyst with the highest manganese content. Weak cubic phase Mn_2O_3 diffraction peak (2θ value = 32.9º; PDF#01-089-2809) existed in the XRD patterns of catalysts with lower manganese content such as [(8Ni1Mn)4(2La8Zr) and (6Ni1Mn)4(2La8Zr)], which indicated a good distribution of manganese oxidate on surface of carrier. Stronger cubic phase Mn_2O_3 diffraction peak (2θ value = 32.9º; PDF#01-089-2809) existed in XRD patterns of catalysts with higher manganese content such as (4Ni1Mn)4(2La8Zr) and (2Ni1Mn)4(2La8Zr), while XRD patterns of (1Ni1Mn)4(2La8Zr) catalyst with the highest manganese content showed no characteristic diffraction peaks of manganese oxidates such as Mn_2O_3, but the cubic phase $Mn_{0.994}Mn_{2.001}O_4$ (2θ value = 36.1º; PDF#01-070-9110) diffraction peak which similar to Mn_3O_4 crystalline phase appeared.

After reductive activation and having been used in steam reforming of ethanol, these five catalysts' XRD patterns were shown in Fig. 1(B): No characteristic diffraction peaks of NiO, but the cubic phase Ni diffraction peaks (2θ value = 44.4, 51.8º; PDF#65-0380) were found in the XRD patterns of all catalysts and the value of Ni diffraction peak reduced with the decrease of Ni content. It indicated that nickel component species of the catalysts existed in the steam reforming of ethanol were in the state of zero-valence[13]. But no diffraction peaks of manganese species were found in XRD patterns of catalysts with lower manganese content such as (8Ni1Mn)4(2La8Zr), (6Ni1Mn)4(2La8Zr) and (4Ni1Mn)4(2La8Zr), which indicated that manganese species were highly dispersed on surface of the carrier. Diffraction peak of cubic phase MnO of certain intensity (2θ value = 40.9º; PDF#01-071-4748) were shown in XRD patterns of (2Ni1Mn)4(2La8Zr) and (1Ni1Mn)4(2La8Zr) catalysts which have higher manganese content.

In ethanol steam reforming, nickel species in all Ni-Mn/La_2O_3-ZrO_2 catalysts obtained through reductive activation existed in the form of cubic phase of nickel, while manganese species existed in the forms of cubic phase MnO. This conclusion can also be confirmed by temperature programmed reduction experimental results.

Catalytic temperature programmed reduction (TPR) characterization: The H_2-TPR characterization results of several catalysts are presented in Fig. 2. In Fig. 2(A)-a, it can be observed that the single active component (1Mn)4(2La8Zr) catalyst has two hydrogen consumption peaks at around 659 and 1019 K, which can, respectively correspond to the $Mn_2O_3 \rightarrow MnO$ and $MnO \rightarrow Mn$ reaction. It is in good aggrement with the reported literature[14,15]. Fig. 2(A)-b showed hydrogen consumption peaks of (1Ni)4(2La8Zr) catalyst existed in three temperature ranges. There was only the rhombohedral phase of NiO in XRD pattern of fresh (1Ni)4(2La8Zr) catalyst, so the three hydrogen consumption peaks in that temperature programmed reduction curve should be assigned to the reductions of three existential state NiO. Of which the peak at 573-673 K can be attributed to the reduction of NiO which was highly dispersed on the surface of the carrier and the peak at 673-873 K was the reduction of NiO which has certain interaction with carrier, while the peak near 908 K can be assigned to the reduction of $NiO \rightarrow Ni$ which interacted with carrier strongly or the reduction of Ni^{2+} which entered into carrier lattice. This result was consistent with that reported in literature[16-18].

The H_2-TPR patterns of bicomponent Ni-Mn/La_2O_3-ZrO_2 catalysts are presented in Fig 2(B). (8Ni1Mn)4(2La8Zr) catalyst's hydrogen consumption peaks appeared at 679, 828 and 1018 K; (6Ni1Mn)4(2La8Zr) catalyst's hydrogen consumption peaks appeared at 694, 816 and 1013 K; (4Ni1Mn)4(2La8Zr) catalyst's appeared at 618 and 812 K; (2Ni1Mn)4(2La8Zr) catalyst's reduction peaks appeared at around 633, 790 and 870 K; (1Ni1Mn)4(2La8Zr) catalyst's hydrogen consumption peaks appeared at 641 and 878 K. Among these peaks, reduction peak at 573-673 K can be attributed to the $Mn_2O_3 \rightarrow MnO$ reaction; peak at 673-923 K came along with the reductive reduction of $NiO \rightarrow Ni$; while

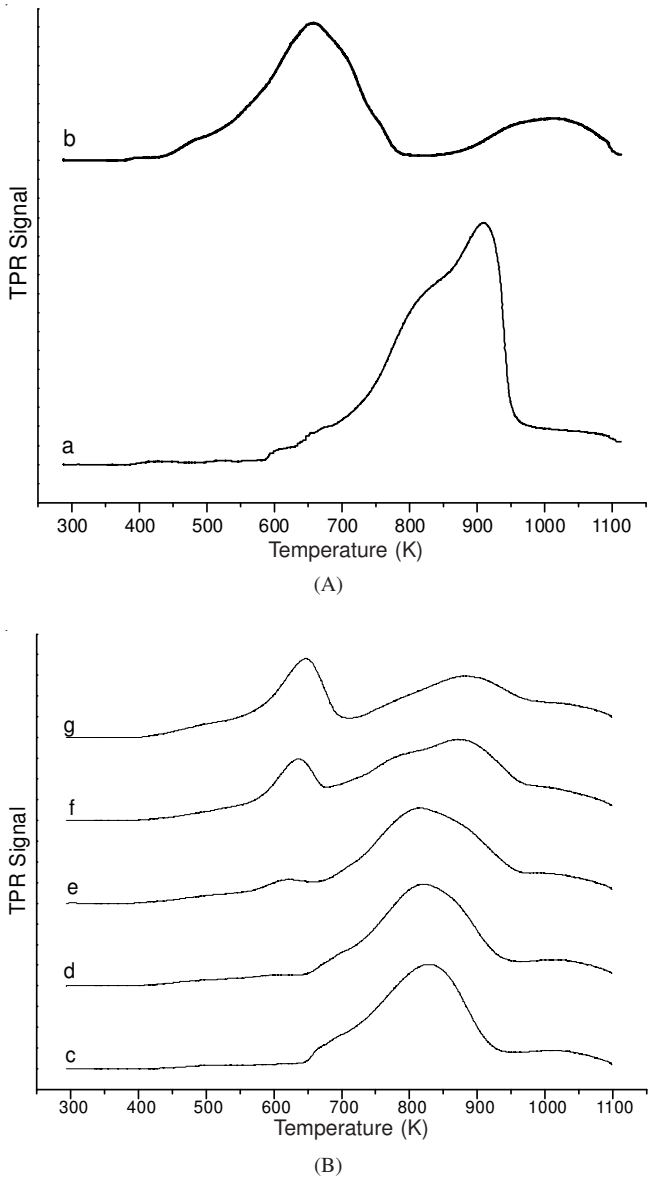

Fig. 2. TPR patterns of Ni-Mn/La_2O_3-ZrO_2 fresh catalysts. a (1Ni)4(2La8Zr) catalyst, b (1Mn)4(2La8Zr) catalyst, c (8Ni1Mn)4(2La8Zr) catalyst, d (6Ni1Mn)4(2La8Zr) catalyst, e (4Ni1Mn)4(2La8Zr) catalyst, f (2Ni1Mn)4(2La8Zr) catalyst, g (1Ni1Mn)4(2La8Zr) catalyst

weak peak near 1020 K can be assigned to the MnO→Mn reduction process[15]. By analyzing patterns in Fig 2, it is concluded that the reduction temperatures of Mn_2O_3→MnO or NiO→Ni in bicomponent Ni-Mn/La_2O_3-ZrO_2 catalysts were slightly lower when compared single component catalysts. It indicated that the dispersion and reducing activity of active species were improved resulting from the coexistence of nickel component and manganese component. The Mn_2O_3→MnO reduction peak area became larger with the increasing content of manganese active component, while the NiO→Ni reduction peak area decreased with the reducing content of nickel active component. The reduction peak areas of species is directly proportional to their content, which indicated nickel and manganese species dispersed preferably on the surface of the carrier.

Catalytic temperature programmed oxidation (TPO) characterization: Temperature programmed oxidation patterns of Ni-Mn/La_2O_3-ZrO_2 catalysts having had continuous catalytic ethanol steam reforming, respectively in the following situations: 523, 573, 623, 673, 723, 773, 823 and 873 K, then had argon blowing were presented in Fig. 3. In Fig. 3, we found that there exist carbon deposition phenomena in ethanol steam reformings having the five Ni-Mn/La_2O_3-ZrO_2 catalysts. The form and amount of the carbon deposition were involved with nickel/manganese ratio as well as reforming temperature. The analytical results were as follows: (8Ni1Mn)4(2La8Zr), (6Ni1Mn)4(2La8Zr), (4Ni1Mn)4(2La8Zr) and (2Ni1Mn)4 (2La8Zr) catalysts all have the following three forms of carbon deposition namely amorphous carbon, fibrous carbon and graphite carbon. According to previous research results[19-23], oxygen consumption peaks appeared below 773 K could be assigned to the oxidation of amorphous carbon; peaks appears at around 873 K due to oxidation of fibrous carbon and the oxidation peak of graphite carbon appeared at 973 K. All the curves abcd in Fig. 3 existed obvious negative peak at around 923 K, which can be speculated to be the result of some certain gas with large thermal conductivity produced from oxidation process of carbon deposition (the formation mechanism and structure still need further research). Moreover, the area of negative peak has something to do with nickel/manganese ratio in catalysts. Temperature programmed oxidation pattern of (1Ni1Mn)4(2La8Zr) catalyst with the highest manganese content presented in Fig. 3e showed no negative peak phenomena.

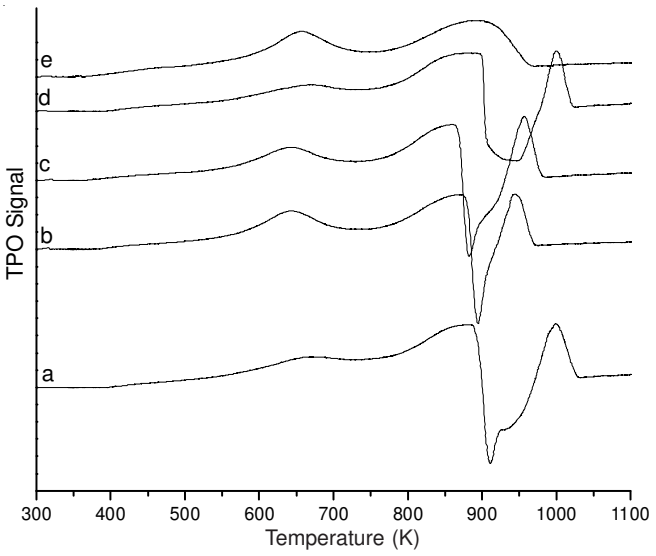

Fig. 3. TPO patterns of Ni-Mn/La_2O_3-ZrO_2 used. a (8Ni1Mn)4(2La8Zr) used b (6Ni1Mn)4(2La8Zr) used, c (4Ni1Mn)4(2La8Zr) used d (2Ni1Mn)4(2La8Zr) used, e (1Ni1Mn)4(2La8Zr) catalyst used

Effect of Ni/Mn ratio on catalytic performance: Make catalysts (8Ni1Mn)4(2La8Zr), (6Ni1Mn)4(2La8Zr), (4Ni1Mn)4(2La8Zr), (2Ni1Mn)4(2La8Zr), (1Ni1Mn)4 (2La8Zr) used in ethanol steam reforming and the results showed that nickel/manganese ratio in catalyst had obvious influence on catalytic activity and selectivity. H_2, CO_2, CO and CH_4 are gaseous products, while acetaldehyde and acetone are liquid products. No ethylene existed in catalysates, which means adding in La_2O_3 alkaline earth metals may ameliorate the catalytic product composition[24].

In Fig. 4 we could find, in temperature interval of 523-823 K, ethanol conversion rate of all catalysts showed a gradual

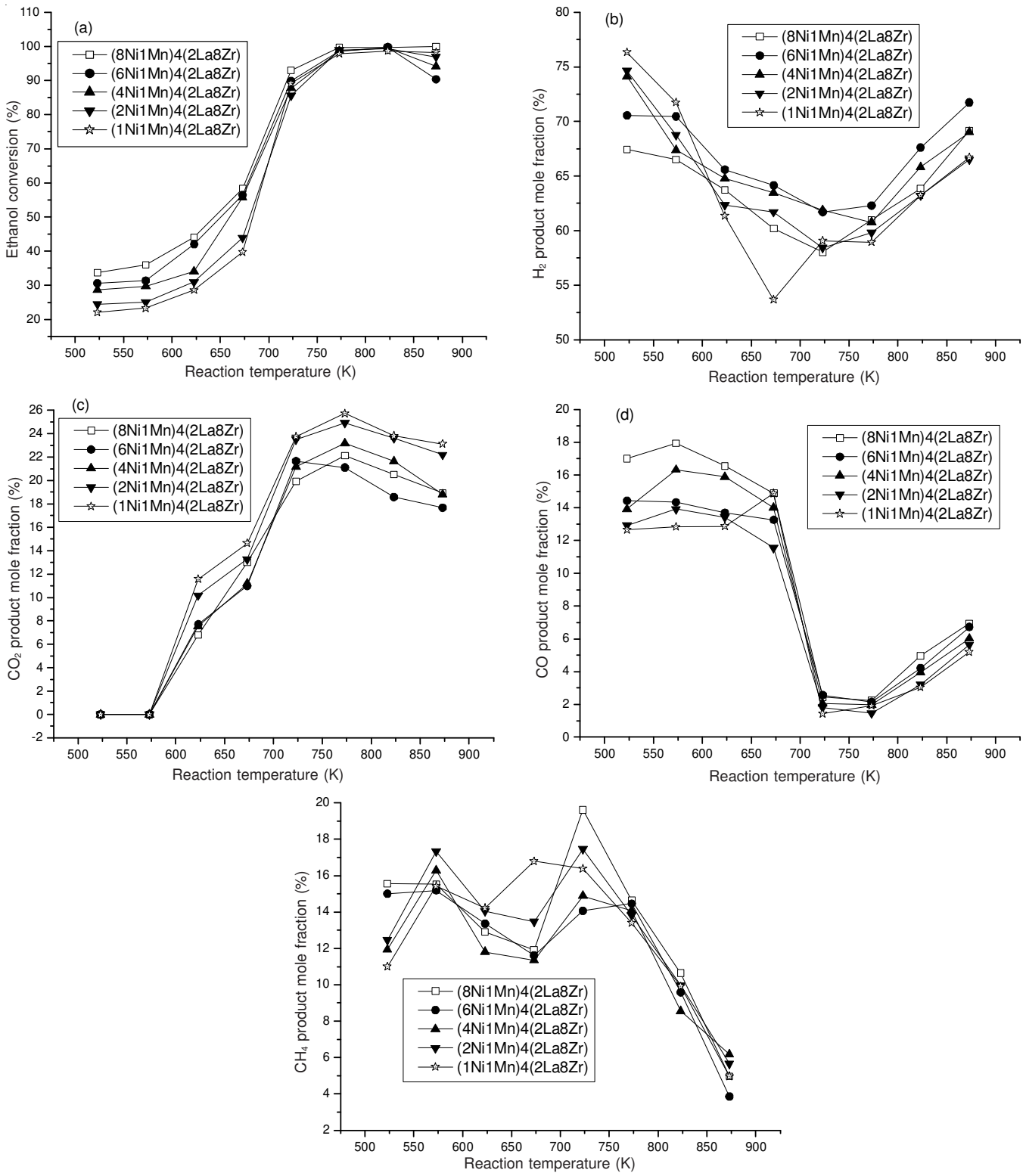

Fig. 4. Influence of Ni:Mn mole ratio on catalytic activity

upward trend (the rate can be 98-100 % at 823 K). When T ≤ 823 K, at the same temperature, ethanol conversion rate increased with the nickel/manganese ratio (increased from 1:1 to the final 8:1) and the increasing nickel in active component contributed to improvement of the ethanol conversion rate and reduce the reaction temperature. When temperature arrived to the highest 873 K, all catalysts came about inactivation in different degrees (such as the decrease of ethanol conversion rate) except (8Ni1Mn)4(2La8Zr) catalyst, of which (6Ni1Mn)4(2La8Zr) and (4Ni1Mn)4(2La8Zr) inactivated even more serious. Fig. 4(d) illustrated that, the Ni:Mn ratio had impacted on gaseous product CO. Catalysts with relatively high Ni content such as (8Ni1Mn)4(2La8Zr), (6Ni1Mn)4 (2La8Zr) and (4Ni1Mn)4(2La8Zr) enhanced the decomposition of ethanol at low temperature. It contained higher content of CH_4 and CO, which resulted from higher ability in breaking C-C bond

of nickel component[3,4]. The ethanol reforming reaction and CO water gas switch aggravated along with the temperature's rising to 773 K. Hence, CO came from decomposition and acetonation of ethanol generated CO_2 through WGS reaction and the content of CO dropped to 2 %, which was consistent with Fig. 4(c). In it, CO product percentage reached its maximum at 773 K. It can also be observed in Fig. 4(c) that the CO content was lower (below 2 %) on (2Ni1Mn)4(2La8Zr) and (1Ni1Mn)4(2La8Zr) catalyst in which manganese content were higher, which indicated that the addition of manganese species led to decrease of CO content which is one kind of harmful products.

Conclusion

The La_2O_3-ZrO_2 composite oxide support prepared by oxalate precipitation method and Ni-Mn/La_2O_3-ZrO_2 catalysts prepared by impregnation were remarkable tetragonal phase. Catalysts exhibited better catalytic activity and selectivity in steam reforming of ethanol and the active component existed in catalysts during the reforming reaction were cubic phase Ni simple substance with zero valence and cubic phase MnO oxide. The dispersion and reductive activity of active components became better, which resulted from the mutual synergy between nickel component and manganese component when they coexisted together. Carbon deposition can be observed on all Ni-Mn/La_2O_3-ZrO_2 catalysts during steam reforming of ethanol; Inactivation phenomenon appeared when reaction temperature is above 873 K.

ACKNOWLEDGEMENTS

This work was supported by Guangxi Natural Science Foundation (Guangxi 0542018).

REFERENCES

1. G. Maggio, S. Freni and S. Cavallaro, *J. Power Sources*, **74**, 17 (1998).
2. A. Tugnoli, G. Landucci and V. Cozzani, *Int. J. Hydrogen Energy*, **33**, 4345 (2008).
3. T.Q. Ye, L.X. Yuan, Y.Q. Chen, T. Kan, J. Tu, X.F. Zhu, Y. Torimoto, M. Yamamoto and Q.X. Li, *Catal. Lett.*, **127**, 323 (2009).
4. F.G. Wang, Y. Li, W.J. Cai, E.S. Zhan, X.L. Mu and W.J. Shen, *Catal. Today*, **146**, 31 (2009).
5. K. Faungnawakij, N. Shimoda, T. Fukunaga, R. Kikuchi and K. Eguchi, *Appl. Catal. A: Gen.*, **341**, 139 (2008).
6. A. Bampenrat, V. Meeyoo, B. Kitiyanan, P. Rangsunvigit and T. Rirksomboon, *Appl. Catal. A: Gen*., **373**, 154 (2010).
7. R. Nedyalkova, A. Casanovas, J. Llorca and D. Montane, *Int. J. Hydrogen Energy*, **34**, 2591 (2009).
8. J.A. Torres, J. Llorca, A. Casanovas, M. Dominguez, J. Salvado and D. Montane, *J. Power Sources*, **169**, 158 (2007).
9. X. Zhou, M. Meng, Z. Sun, Q. Li and Z. Jiang, *Chem. Eng. J*., **174**, 400 (2011).
10. J. Papavasiliou, G. Avgouropoulos and T. Ioannides, *Appl. Catal. B: Environ.*, **66**, 168 (2006).
11. A. Casanovas, C. de Leitenburg, A. Trovarelli and J. Llorca, *J. Chem. Eng*., **154**, 267 (2009).
12. A. Berman, R.K. Karn and M. Epstein, *Appl. Catal. A: Gen*., **282**, 73 (2005).
13. J.D.A. Bellido, J.E. De Souza, J.-C. M'Peko and E.M. Assaf, *Appl. Catal. A: Gen*., **358**, 215 (2009).
14. J. Papavasiliou, G. Avgouropoulos and T. Ioannides, *J. Catal*., **251**, 7 (2007).
15. R. Lin, W.P. Liu, Y.J. Zhong and M.F. Luo, *Appl. Catal. A: Gen*., **220**, 165 (2001).
16. H. Jeong and M. Kang, *Appl. Catal. B: Environ*., **95**, 446 (2010).
17. J.D.A. Bellido, E.Y. Tanabe and E.M. Assaf, *Appl. Catal. B: Environ*., **90**, 485 (2009).
18. J.D.A. Bellido and E.M. Assaf, *Appl. Catal. A: Gen*., **352**, 179 (2009).
19. H. Wang, Y. Liu, L. Wang and Y.N. Qin, *Chem. Eng. J.*, **145**, 25 (2008).
20. A. Fatsikostas, *J. Catal*., **225**, 439 (2004).
21. S.M. de Lima, A.M. da Silva, L.O.O. da Costa, J.M. Assaf, G. Jacobs, B.H. Davis, L.V. Mattos and F.B. Noronha, *Appl. Catal. A: Gen.*, **377**, 181 (2010).
22. L.O.O. da Costa, A.M. da Silva, F.B. Noronha and L.V. Mattos, *Int. J. Hydrogen Energy*, **37**, 5930 (2012).
23. S.M. de Lima, A.M. da Silva, L.O.O. da Costa, U.M. Graham, G. Jacobs, B.H. Davis, L.V. Mattos and F.B. Noronha, *J. Catal*., **268**, 268 (2009).
24. L.F. Zhang, Y.P. Wang and Q.W. Huang, *Chem. Ind. Eng. Progr*., **27**, 1605 (2008).